Available online at www.sciencedirect.com

SciVerse ScienceDirect

Ceramics International 39 (2013) 1539–1545

CERAMICS INTERNATIONAL

www.elsevier.com/locate/ceramint

Study of electrical transport properties of Eu^{+3}substituted MnZn-ferrites synthesized by co-precipitation technique

M. Asif Iqbal, Misbah-ul-Islam*, Irshad Ali, Hasan M. Khan, Ghulam Mustafa, Ihsan Ali

Department of Physics, Bahauddin Zakariya University, Multan 60800, Pakistan

Received 6 June 2012; received in revised form 31 July 2012; accepted 31 July 2012
Available online 7 August 2012

Abstract

Eu substituted MnZn-ferrites with nominal composition $Mn_{0.78}Zn_{0.22}Eu_x\ Fe_{(2-x)}O_4$ ($x=0.0$, 0.02, 0.04, 0.06, 0.08 and 0.10) were prepared by co-precipitation technique. The effect of Europium substitution on electrical transport properties of Mn–Zn ferrites is reported. XRD analysis reveals fcc phase in all the samples along with few traces of second phase. The lattice constant shows decreasing trend with the substitution of Eu due to partial solubility of Eu-ions in the lattice. Room temperature resistivity both at 10 and 20 V shows on average an increasing trend. This increase in resistivity is attributed to the unavailability of Fe^{+3} ions in the lattice due to Eu-substitution. The dc resistivity decreases with temperature for all the samples at 10 V and 20 V indicating the semiconducting behavior of these samples. Room temperature dc resistivity and activation energies show similar trend both at 10 V and 20 V indicating that the samples with high resistivity have high activation energies and vice versa. The dielectric constant (ε'), complex dielectric constant (ε'') and loss tangent of these samples decreased with the increase of Eu-concentration, following the Maxwell–Weigner model.

Keywords: Ferrites; Wet method; Resistivity; Dielectric constant

1. Introduction

Ferrites have been studied extensively owing to their vast applications, especially in magnetic memories, high frequency circuits, transformer cores and analog devices [1,2]. Trends in ferrite technology in the days to come includes challenges in applications, advancement in manufacturing techniques and cost factor in both commercial and defense applications. Broad band operation at millimeter and sub-millimeter wave length levels will be required in future space and satellite interconnects. A special application of MnZn-ferrites is found in the absorption of radar signals, which is the basis of stealth technology. Moreover, by introducing a relatively small amount of RE, an important modification of both the structure, and magnetic and electrical properties can be observed in these ferrites which has attracted the attentions of researchers [3].The influence of RE ions like Eu^{3+} on magnetic properties of ferrites have already been reported by different researchers [11]. In this paper, efforts are made to investigate the effect of RE ions (Eu^{3+}) on the electrical properties of Mn–Zn ferrites.

2. Experimental technique

The co-precipitation method was used to prepare $Mn_{0.78}Zn_{0.22}Eu_xFe_{(2-x)}O_4$($x=0.0$, 0.02, 0.04,0.06,0.08 and 0.1) ferries. Metal chlorides like $ZnCl_2$, $FeCl_3$, $MnCl_2\cdot 4H_2O$ and Eu_2O_3(99.99% pure) were used as starting materials. Where NaOH and Na_2CO_3 were used as precipitating agent. Stoichometric amount of each chloride was dissolved in 100 ml of de-ionized water. Eu_2O_3 was first dissolved in HCl by heating up to 60 °C in a beaker and continuously stirred by a magnetic stirrer. All the prepared solutions were mixed in 1000 ml beaker. The beaker was put on a magnetic stirrer with hot plate material at 35–45 °C. Precipitating agents $NaOH/Na_2CO_3$ (1:1) were heated at 40 °C and stirred for a while. The $NaOH/Na_2CO_3$ were poured slowly into the prepared solution, as a result brown precipitates formed and settled

*Corresponding author. Fax: +92 061 9210068.
E-mail address: muislampk@yahoo.com (Misbah-ul-Islam).

0272-8842/$ - see front matter © 2012 Elsevier Ltd and Techna Group S.r.l. All rights reserved.
http://dx.doi.org/10.1016/j.ceramint.2012.07.104

at the bottom. The prepared solution was stirred continuously for 2 h. The pH was maintained between eight and nine. The precipitates were settled and filtered by a filter paper placed on a suction flask operating on a water pump. These precipitates also contain chlorides which were eliminated by washing the precipitates with de-ionized water several times. The removal of chloride ions was checked by the $AgNO_3$ test until removal of all chlorides were ensured. The precipitates were then dried at 100 °C for 24 h in an oven. The dried precipitates were ground until they were converted into powder. The powder was then pressed into pellets under the load of (~30 kN) by using the Paul–Otto Weber Hydraulic Press. The pellets were pre-sintered in a digital electric box furnace at temperature 1000 °C for 5 h, then at 1150 °C for 4 h and finally sintered at 1300 °C for 3 h followed by furnace cooling. The XRD was taken on X-ray diffractometer, equipped with CuK_α radiations. The 2θ scanning range was 20–70°.The dielectric measurements were taken on an LCR meter Model 8101 Gw INSTEK.The electrical resistivity was measured by the two probe method. A Keithly source meter model-197 was used for the said purpose.

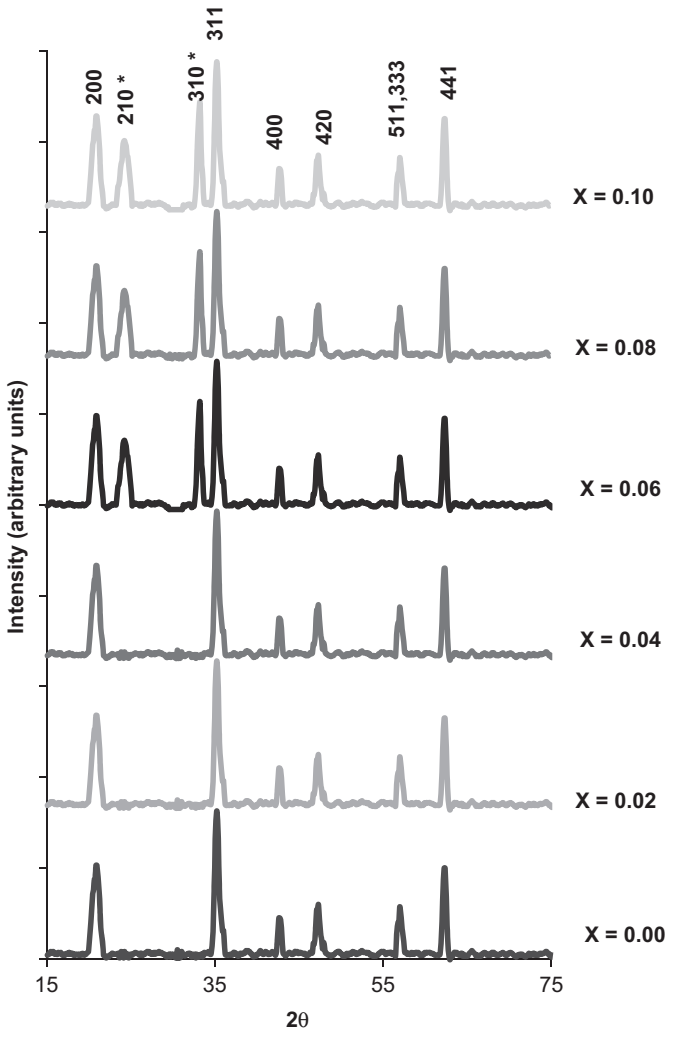

Fig. 1. XRD patterns for $Mn_{0.78}Zn_{0.22}Eu_xFe_{(2-x)}O_4$($x$=0.00, 0.02, 0.04, 0.06, 0.08 and 0.10) ferrites.

3. Results and discussion

3.1. X-ray diffraction

Fig. 1 shows X-ray diffraction patterns of the $Mn_{0.78}Zn_{0.22}Eu_xFe_{(2-x)}O_4$ (x=0.0, 0.02, 0.04, 0.06, 0.08 and 0.10) ferrites. It is observed that the samples $0 \le x \le 0.04$ revealed fcc single phase where as rest of the three samples (x=0.06–0.10) reflected biphasic trend. For x=0.00–0.04, seven well defined diffraction peaks were observed. Secondary peaks were observed at 2θ=23.1 and 33.3θ (indicated by *).These peaks can be identified as $EuFeO_3$ reflection matched with ICDD PDF#741475. The secondary phase on the grain boundaries appears due to high reactivity of Fe^{3+} with Eu^{3+}[4].

3.1.1. Lattice constants

Fig. 2 shows a plot of lattice constant vs. Eu-content. Lattice constant increases with the increase of Eu substitution up to x=0.04. The increase in lattice constant is due to the partial incorporation of the Eu contents into the spinel lattice as the Eu ion has the ionic radius (0.947 Å), larger than the ionic radius of Fe^{3+}(0.645 Å) [5]. At $x > 0.04$, the lattice constant decreases. This may be

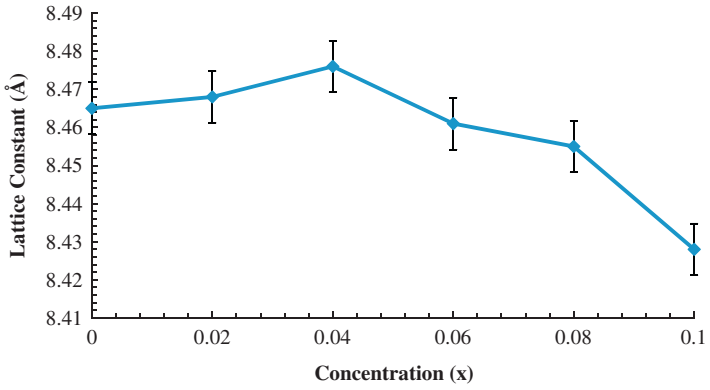

Fig. 2. Lattice constant (Å) vs. Eu concentration (x) for $Mn_{0.78}Zn_{0.22}Eu_xFe_{(2-x)}O_4$ (x=0.00, 0.02, 0.04, 0.06, 0.08 and 0.10) ferrites.

attributed to the segregation of the Eu ions at the grain boundaries. It may be possible that due to the differences in the thermal expansion coefficients, spinel lattice is compressed by the intergranular secondary phase [5]. Hence a decrease in lattice constant with increasing concentration of Eu may suggest the existence of a solubility limit for Eu ions. Hence small amount of Eu introduced in $Mn_{0.78}Zn_{0.22}Fe_2O_4$ ferrite affects not only the phase composition but also the size of the spinel matrix.

3.1.2. X-ray density, bulk density and porosity

X-ray density (D_x) of the present samples were calculated from X-ray diffraction analysis by using the relation [6]

$$D_x = 8M/Na^3 \quad (1)$$

where M is the molecular weight of the sample, N is the Avogadro number and a^3 is the cell volume.

The bulk density (D_s) was measured by the Archimedes principle using toluene, according to the formula;

$$D_s = (W_s/W_t)p_t \quad (2)$$

where W_s denotes weight of the specimen in air, W_t is the apparent weight loss in toluene and p_t is the density of toluene = 0.857 g/cc.

The influence of Eu^{3+} concentration on X-ray density (D_x) and physical density (D_s) is shown in Fig. 3. X-ray density exhibits an increasing trend from 4.693 to 4.941 g/cm^3 with the increase of Europium contents as it mainly depends upon the molecular weight and lattice constant of the samples. The physical density also increases with Europium contents from 4.165 to 4.524 g/cm^3 which is attributed to the difference in atomic weight of Europium (151.965 amu) and iron (55.845 amu). Moreover the presence of Eu^{3+} ions activates the sintering process in ferrites and leading to increase in densities [7]. The large values of X-ray density (D_x) than bulk density (D_s) may be due to existence of pores in the samples [8].

Since the formation of secondary phase ($EuFe_2O_3$) fills inter-granular voids and exhibits good densification, a decrease in porosity was expected with Europium contents [3] as shown in Fig. 4.

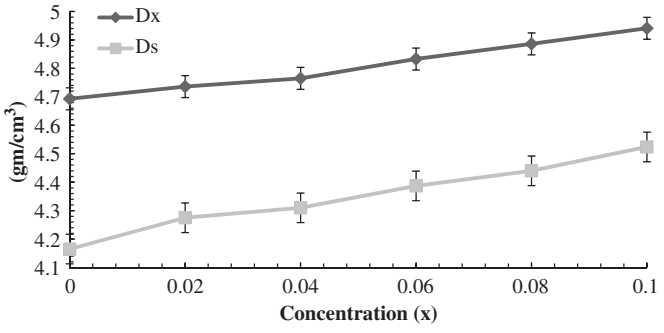

Fig. 3. X-ray/bulk densities (g/cm^3) vs. Eu-concentration (x) for $Mn_{0.78}Zn_{0.22}Eu_xFe_{(2-x)}O_4$ (x=0.00, 0.02, 0.04, 0.06, 0.08 and 0.10) ferrites.

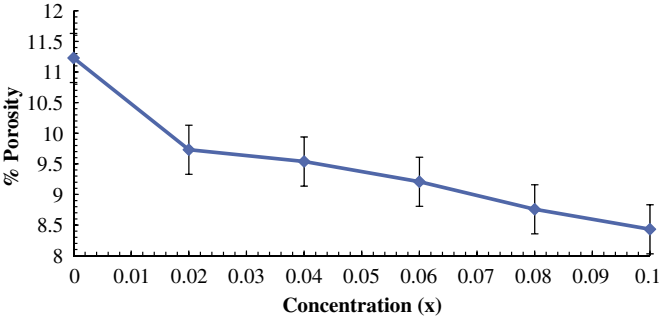

Fig. 4. % Porosity vs. Eu-concentration (x) for $Mn_{0.78}Zn_{0.22}Eu_xFe_{(2-x)}O_4$ (x=0.00, 0.02, 0.04, 0.06, 0.08 and 0.10) ferrites.

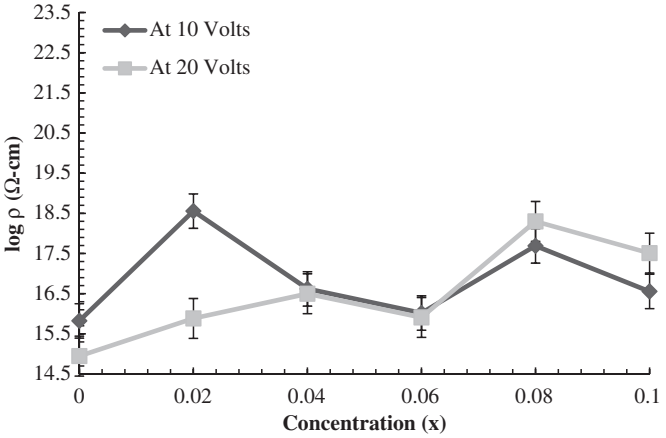

Fig. 5. Log ρ (Ω cm) vs. Eu-concentration (x) for $Mn_{0.78}Zn_{0.22}Eu_xFe_{(2-x)}O_4$ (x=0.00, 0.02, 0.04, 0.06, 0.08 and 0.10) ferrites at 10 and 20 V.

3.2. Electrical properties

3.2.1. Room temperature resistivity

Fig. 5 shows the variation of Log ρ vs. Eu-concentration at 10 and 20 applied voltages respectively. On average, it was observed that the room temperature resistivity increases with the increase of Eu-content from 4.86×10^6 to 4.37×10^7 Ω-cm at 10 V and from 6.48×10^6 to 7.32×10^7 Ω-cm at 20 V, this behavior is attributed to the field effect. Owing to large ionic radius of Eu (0.947 Å) as compared to Fe^{3+} (0.645 Å), it has been reported that Eu ions occupy octahedral sites [9]. The concentration of Fe^{3+} ions gradually decreases at B-sites when Eu is substituted in place of iron. The hopping rate of electron transfer will decrease with the decrease of Fe^{3+} ions concentration. As a result, it enhances the dc resistivity with the increase of Eu concentration. The Fe^{2+} ions' concentration is a characteristic property of a given material and it depends upon the several factors namely amount of substituent, sintering temperature, atmosphere, time and grain size etc. [10]. Another possible reason for increase in resistivity on increasing Eu is due to the fact that the occupation of Eu ions at B-sites will increase the separation between Fe^{3+} and Fe^{2+} ions in proportion to its ionic radius which is consistent with the variation of lattice constant vs.

Eu-content. Since the hopping of electrons between ferrous and ferric ions is restricted hence both resistivity and activation energy increases. These results are consistent with the results reported by various authors [3,5]. The possible conduction mechanism in the present samples may be due to hopping of electrons from Fe^{2+} to Fe^{3+} and hole transfer from Mn^{3+} to Mn^{2+} ions [11,12]:

$$Fe^{2+} \Leftrightarrow Fe^{3+} + e^{-}$$

$$Mn^{3+} + e^{-} \Leftrightarrow Mn^{+2}$$

Combining the above two equations,

$$Mn^{2+} + Fe^{3+} \Leftrightarrow Mn^{3+} + Fe^{2+}$$

The possible reason for the decrease in resistivity in these ferrites may be due to the presence of Fe^{2+} ions produced during sintering process.

3.2.2. Temperature dependent DC resistivity

Temperature dependant dc resistivity at two different voltages (10 and 20 V) was measured in the temperature range 30–210 °C. The Arrhenius plots at both voltages are shown in Fig. 6 (a) and (b). The dc resistivity decreases linearly with temperature for all the samples indicating the semiconducting behavior of these samples. It was observed from these plots that with the increase in voltage, the magnitude of temperature dependent resistivity for all the samples decreased due to field effect. The steeper slope for all the samples can be attributed to thermally activated mobility of charge carriers, but not to a thermally activated creation of these carriers. The possibility of occurrence of hopping conductivity in ferrites has been established in literature, considering the small polaron model. Thus, it has been concluded that at higher temperatures small polaron hopping mechanism may be the likely mechanism [6]. The observed decrease in dc resistivity with temperature is normal behavior for semiconductors which follows the Arrhenius relation [3].

3.2.3. Activation energy

The activation energies were calculated from the slope of the Arrhenius plots at two different voltages (10 and 20 V) and are plotted in Fig. 7. It is found that the activation energy and the electrical resistivity vs. Eu concentration show similar behavior. It is also observed that the sample with higher resistivity has higher values of activation energies and vice versa [13].

Due to the substitution of Eu ions, the higher values of activation energies at higher Europium concentration show the strong blocking of the conduction mechanism between ferrous and ferric ions. A logical approach for the increasing behavior of activation energy can be attributed to the increase in lattice constant. It has been reported that in ferrites, the inter-ionic distance increases with the increase in the values of lattice constant [14]. This gradual increase in inter-ionic distance enhances the barrier height encountered by the charge carriers and enhances the activation energy, subsequently [6].

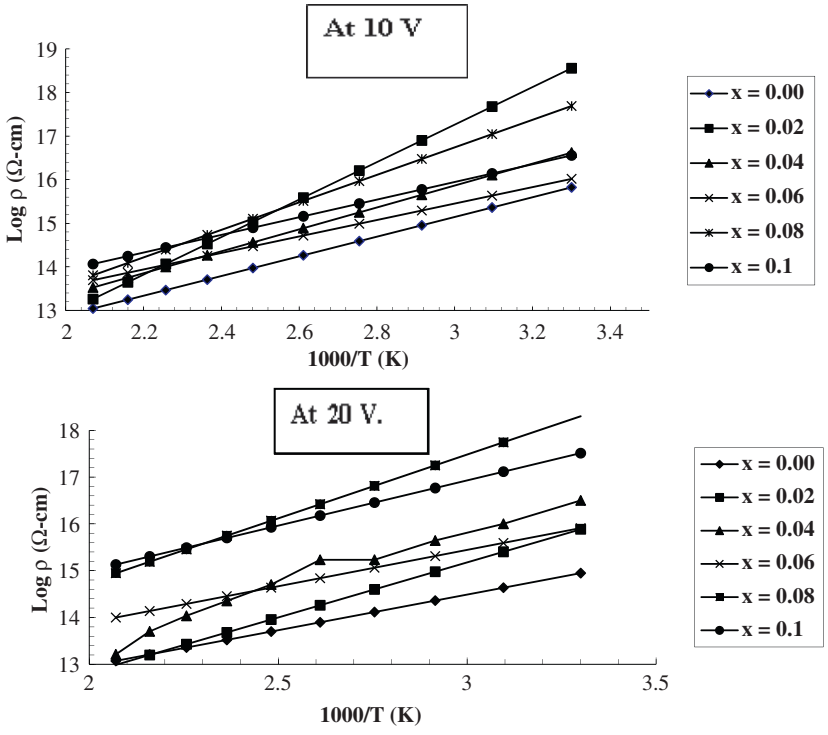

Fig. 6. (a) $1000/T$ (K^{-1}) vs. log ρ (Ω-cm) for $Mn_{0.78}Zn_{0.22}Eu_xFe_{(2-x)}O_4$ (x=0.00, 0.02, 0.04, 0.06, 0.08 and 0.10) ferrites at 10 V. (b) $1000/T$ (K^{-1}) vs. log ρ (Ω-cm) for $Mn_{0.78}Zn_{0.22}Eu_xFe_{(2-x)}O_4$ (x=0.00, 0.02, 0.04, 0.06, 0.08 and 0.10) ferrites at 20 V.

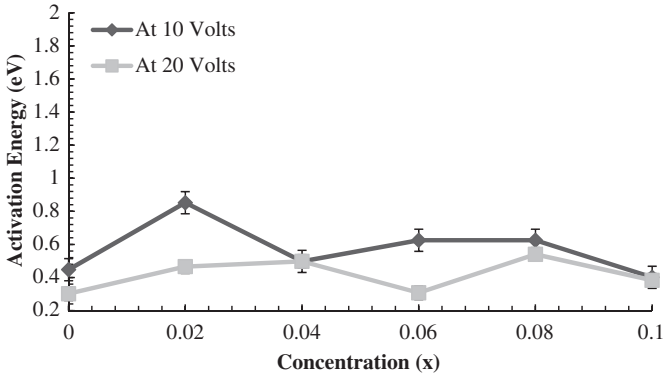

Fig. 7. Activation energy (eV) vs. Eu-concentration (x) at 10 and 20 V for $Mn_{0.78}Zn_{0.22}Eu_xFe_{(2-x)}O_4$ (x=0.00, 0.02, 0.04, 0.06, 0.08 and 0.10) ferrites.

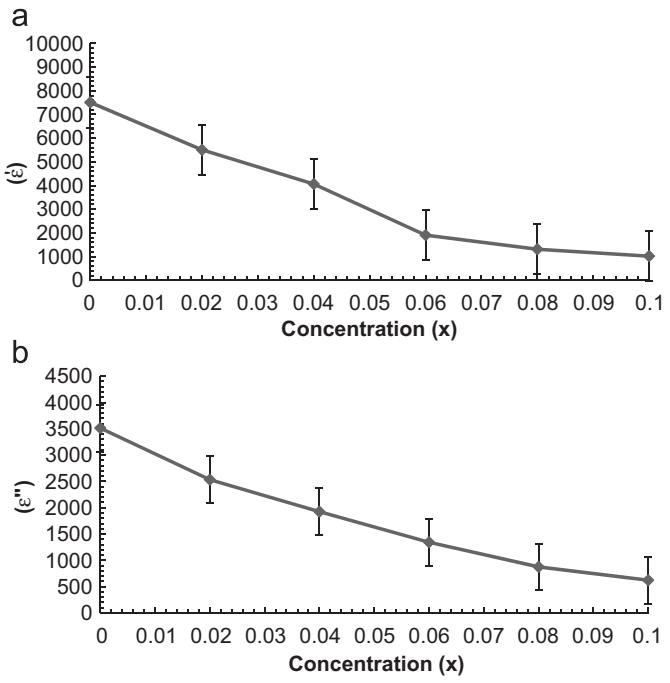

Fig. 8. (a) Dielectric constant (ε') vs. Eu-concentration (x) for $Mn_{0.78}Zn_{0.22}Eu_xFe_{(2-x)}O_4$ (x=0.00,0.02,0.04,0.06,0.08 and 0.10) ferrites. (b) Complex dielectric constant (ε'') vs. Eu-concentration (x) for $Mn_{0.78}Zn_{0.22}Eu_xFe_{(2-x)}O_4$ (x=0.00, 0.02, 0.04, 0.06, 0.08 and 0.10) ferrites.

3.3. Dielectric properties

3.3.1. Compositional effect on dielectric and complex dielectric constant

The variation of dielectric constant (ε') and complex dielectric constant (ε''), determined at the frequency in kilohertz at room temperature are shown in Fig. 8(a) and (b) respectively. Both and ε'' decrease with the increase of Europium concentration as the mechanism for the electrical conduction is similar to that of the dielectric polarization. It was observed that the electronic exchange between $Fe^{2+} \leftrightarrow Fe^{3+}$ results in local displacements, determining the polarization of the ferrites. Thus, it is the number of ferrous ions on octahedral sites that play a dominant role in the processes of conduction as well as dielectric polarization. Due to its larger ionic radius, Eu^{3+} ions will prefer to occupy octahedral sites [15]. The concentration of Fe^{3+} ions at B-sites decreases gradually with increasing concentration of Europium. The reduction in the values of dielectric constant and complex dielectric constant with increasing concentration of Europium is due to depicting concentration of iron ions at B-sites which play a dominant role in dielectric polarization. The electron transfer between Fe^{2+} and Fe^{3+} ions ($Fe^{2+} \leftrightarrow Fe^{3+} + e^-$) hindered the hopping process and hence polarization decreased. Consequently, both dielectric () and complex dielectric constant (ε'') decrease with increasing Europium contents [16].

3.3.2. Effect of frequency on dielectric and complex dielectric constant

Fig. 9 (a) and (b) shows the variation of the real and imaginary part of the dielectric constant as a function of frequency at room temperature for all the samples. It is clear from the figure that both real and imaginary part of dielectric constant show dispersion with frequency. The values of both and ε'' are high at low frequency and then decreases rapidly with the increase in frequency for all the compositions. Ultimately, it attains a constant value which is the general trend for all the ferrite samples [12]. This general behavior depicts the dispersion due to the Maxwell–Wagner type interfacial polarization, in agreement with Koop's phenomenological theory. The phenomenon of electron exchange between Fe^{2+} and Fe^{3+} ions gives local displacement of electrons in the direction of an applied electric field, which subsequently determines the polarization. The polarization decreases substantially with increase in frequency and reaches a constant value due to the fact that beyond a certain frequency of external field, the electron exchange between Fe^{2+} and Fe^{3+} ions cannot follow the alternating field. Moreover, the higher values of dielectric constant observed at lower frequencies are due to the predominance of species like Fe^{2+} ions, due to which interfacial dislocation piles-up oxygen vacancies and grain boundary defects etc. The decrease in both and ε'' with frequency is due to the fact that any species contributing to polarizability is bound to show the lagging behind in the applied field at higher frequencies [12,17–19].

3.3.3. Dielectric loss tangent

The variation of dielectric loss tangent ($\tan\delta$) vs. frequency is shown in Fig. 9c. It is clear from the figure that $\tan\delta$ decreases with increasing Eu concentration. This can be attributed to the increase in resistivity which causes reduction in $\tan\delta$ [20].

When the frequency of the applied ac electric field is much smaller than hopping frequency of electrons between

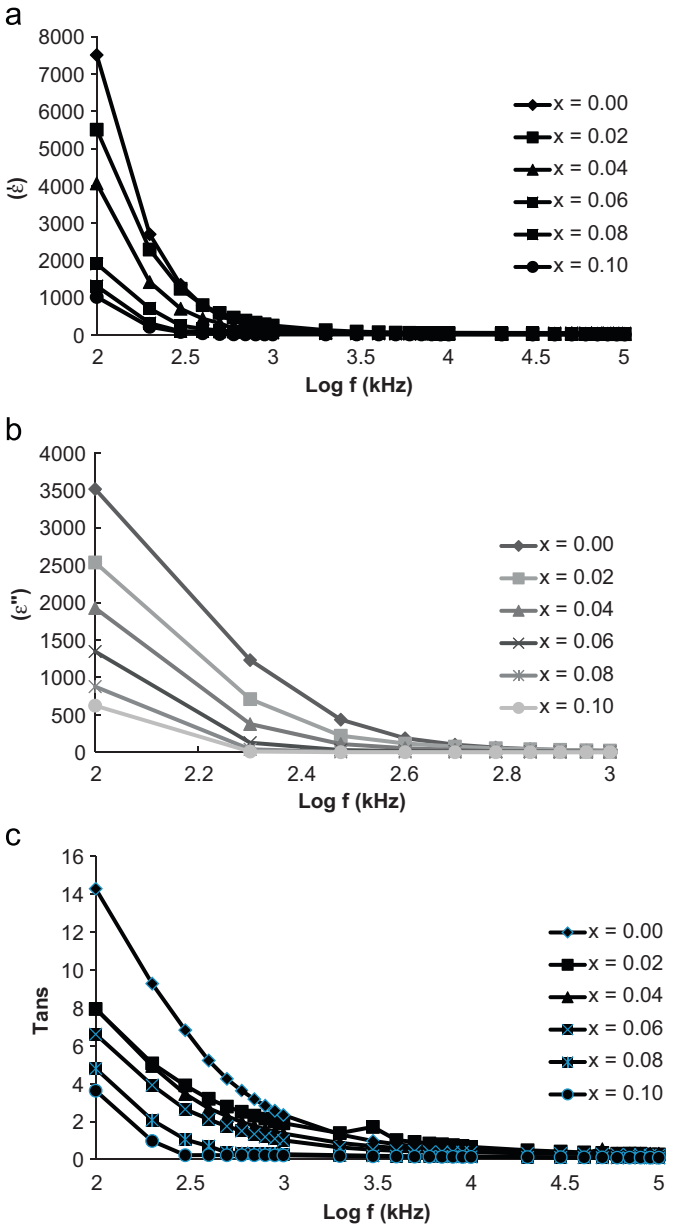

Fig. 9. (a) Dielectric constant () vs. frequency (Hz) for $Mn_{0.78}Zn_{0.22}Eu_xFe_{(2-x)}O_4$ (x=0.00, 0.02, 0.04, 0.06, 0.08 and 0.10) ferrites. (b) Complex dielectric constant (ε'') vs. frequency (Hz) for $Mn_{0.78}Zn_{0.22}Eu_xFe_{(2-x)}O_4$ (x=0.00, 0.02, 0.04, 0.06, 0.08 and 0.10) ferrites. (c) Frequency (Hz) vs. loss tangent for $Mn_{0.78}Zn_{0.22}Eu_xFe_{(2-x)}O_4$ (x=0.00, 0.02, 0.04, 0.06, 0.08 and 0.10) ferrites.

Fe^{2+} and Fe^{3+} ions at adjacent octahedral sites, the electrons follow the field and hence the loss is maximum. At higher frequencies of the applied electric field, the hopping frequency of the electron exchange between Fe^{2+} and Fe^{3+} ions cannot follow the applied field beyond certain critical frequency and the loss is minimum [17]. At low frequency, tan δ is high and decreases rapidly at high frequency. Moreover, ferrites consist of well conducting grains and poorly conducting grain boundaries while thin insulated grain boundaries are more effective at low frequency, however well conducting grain boundaries are more effective at the high frequency region. Hence, it is expected that energy loss is high at the low frequency region while it is low at the high frequency region. Therefore tan δ is high in the low frequency region because more energy is required for the hopping process of charge carriers, whereas it is low in the high frequency region because little energy is required for the hopping process of charge carriers in this region [18,19].

4. Conclusions

XRD analysis showed that the first three samples revealed fcc single phase whereas rest of the three are biphasic. Change in lattice constant at $x > 0.04$ indicates the solubility limit of Eu in the spinel lattice. On average, room temperature resistivity increased with the increase of Eu-content at both the voltages whereas temperature dependent resistivity for all the samples follows the Arrhenius equation. X-ray and bulk densities increase with Eu-contents; however, decreasing trend in porosity was attributed to the substitution of Eu thereby making all samples denser. It is observed that the samples having high resistivity have high activation energy and vice versa. The dielectric constant, complex dielectric constant and loss tangent decreased with the increase of Eu-concentration. The decrease in (ε') and increase in resistivity is required for high frequency applications.

References

[1] Y. Yafet, C. Kittle, Physical Review 37 (2) (1952).
[2] A.H. Morish, The Physical Principles of Magnetism, John Wiley & Sons Publishers, New York, London, Sydney, 1956.
[3] N. Rezlescu, E. Rezlescu, P.D. Popa, L. Rezlescu, Effects of RE oxides on physical properties of Li–Zn ferrite, Journal of Alloys and Compounds (1998) 657–659.
[4] A.B. Gadkari, T.J. Shinde, P.N. Vasmbekar, Structural analysis of Y^{3+}doped Mg–Cd ferrites prepared by co-precipitation method, Materials Chemistry and Physics 114 (2009) 505–510.
[5] N. Rezlescu, E. Rezlescu, C. Pasnicu, M.L. Craus, Effect of rare-earth ions on some properties of a nickel–zinc ferrite, Journal of Physics: Condensed Matter 6 (1994) 5707–5716.
[6] A.A. Sattar, Temperature dependence of electrical resistivity and thermo electric power of RE substituted Cu–Cd ferrite, Egyptian Journal of Solids 26 (2) (2003) 113–121.
[7] M.M. Haquea, M. Huqa, M.A. Hakimb, Densification, magnetic and dielectric behaviour of Cu-substituted Mg–Zn ferrites, Materials Chemistry and Physics 112 (2008) 580–586.
[8] B.P. Rao, K.H. Rao, Distribution of In^{+3} ions in indium-substituted Ni–Zn–Ti ferrites, Journal of Magnetic Materials 292 (2005) 44–48.
[9] N. Rezlescu, E. Rezlescu, The influence of Fe-substitutions by RE ions in a Ni–Zn ferrites, Solid State Communications 88 (1993) 139–141.
[10] U. Ghazanfar, S.A. Siddiqi, G. Abbas, Study of room temperature dc resistivity in comparison with activation energy and drift mobility of NiZn ferrites, Materials Science and Engineering B118 (2005) 132–134.
[11] G.L. Sun, J.B. Li, J.J. Sun, X.Z. Yang, The influence of Zn^{2+} and some rare-earth ions on the magnetic properties of nickel–zinc ferrites, Journal of Magnetism and Magnetic Materials 281 (2004) 173–177.

[12] D. Ravinder, P.V.B. Reddy, High-frequency dielectric behaviour of Li–Mg ferrites, Materials Letters 57 (2003) 4344–4350.
[13] B. Ramesh, D. Ravinder, Electrical properties of Li–Mn ferrites, Materials Letters 62 (2008) 2043–2046.
[14] E. Rezlescu, N. Rezlescu, P.D. Popa, L. Rezlescu, C. Pasnicu, The influence of R_2O_3 (R = Yb,Er, Dy, Tb, Gd, Sm, and Ce) on the electrical and mechanical properties of a nickel–zinc ferrite, Physica Status Solidi A (1997) 672–678.
[15] T.N. Brusentsova, V.D. Kuznetsov, Synthesis and investigation of magnetic properties of substituted ferrite nano particles of spinel system $Mn_{1-x}Zn_x[Fe_{2-y}Ly]O_4$, Journal of Magnetism and Magnetic Materials 311 (2007) 22–25.
[16] T.M. Meaza, S.M. Attiab, A.E. Ataa, Effect of tetravalent titanium ions substitution on the dielectric properties of Co–Zn ferrites, Journal of Magnetism and Magnetic Materials 257 (2003) 296–305.
[17] G.R. Mohan, D. Ravinder, A.V.R. Reddy, B.S. Boyanov, Dielectric properties of polycrystalline mixed nickel–zinc ferrites, Materials Letters 40 (1999) 39–45.
[18] S.F. Mansour, Frequency and composition dependence on the dielectric properties for Mg–Zn ferrite, Egyptian Journal of Solids 28 (2) (2005) 211–214.
[19] Z. Cveji, S. Raki, S. Jankov, S. Skuban, A. Kapor, Dielectric properties and conductivity of zinc ferrite and zinc ferrite doped with yttrium, Journal of Alloys and Compounds 480 (2009) 241–245.
[20] A.M. Shaikh, S.S. Bellad, B.K. Chougule, Temperature and frequency-dependent dielectric properties of Zn substituted Li–Mg ferrites, Journal of Magnetism and Magnetic Materials 195 (1999) 384–390.